Cell Calcium (1998) **23**(5), 291–302

Stochastic simulation of a single inositol 1,4,5-trisphosphate-sensitive Ca^{2+} channel reveals repetitive openings during 'blip-like' Ca^{2+} transients

S. Swillens[1], P. Champeil[2], L. Combettes[3], G. Dupont[4]

[1]Institut de Recherche Interdisciplinaire, Faculté de Médecine, Université Libre de Bruxelles, Bruxelles, Belgium
[2]Unité de Recherche Associée 2096 (Centre National de la Recherche Scientifique) & Section de Biophysique des Protéines et des Membranes, Département de Biologie Cellulaire et Moléculaire (Commissariat à l'Energie Atomique), Centre d'Etudes de Saclay, Gif-sur-Yvette, France
[3]Unité de Recherche U442 (Institut National de la Santé et de la Recherche Médicale), Université de Paris-Sud, Orsay, France
[4]Unité de Chronobiologie Théorique, Faculté des Sciences, Université Libre de Bruxelles, Bruxelles, Belgium

Summary Confocal microscope studies with fluorescent dyes of inositol 1,4,5-trisphosphate ($InsP_3$)-induced intracellular Ca^{2+} mobilization recently established the existence of 'elementary' events, dependent on the activity of individual $InsP_3$-sensitive Ca^{2+} channels. In the present work, we try by theoretical stochastic simulation to explain the smallest signals observed in those studies, which were referred to as Ca^{2+} 'blips' [Parker I., Yao Y. Ca^{2+} transients associated with openings of inositol trisphosphate-gated channels in *Xenopus* oocytes. *J Physiol Lond* 1996; **491**: 663–668]. For this purpose, we assumed a simple molecular model for the $InsP_3$-sensitive Ca^{2+} channel and defined a set of parameter values accounting for the results obtained in electrophysiological bilayer experiments [Bezprozvanny I., Watras J., Ehrlich B.E. Bell-shaped calcium-response curves of $Ins(1,4,5)P_3$- and calcium- gated channels from endoplasmic reticulum of cerebellum. *Nature* 1991; **351**: 751–754; Bezprozvanny I., Ehrlich B.E. Inositol (1,4,5)-trisphosphate ($InsP_3$)-gated Ca channels from cerebellum: conduction properties for divalent cations and regulation by intraluminal calcium. *J Gen Physiol* 1994; **104**: 821–856]. With a stochastic procedure which considered cytosolic Ca^{2+} diffusion explicitly, we then simulated the behaviour of a single channel, placed in a realistic physiological environment. An attractive result was that the simulated channel exhibited bursts of activity, arising from repetitive channel openings, which were responsible for transient rises in Ca^{2+} concentration and were reminiscent of the relatively long-duration experimental Ca^{2+} blips. The influence of the values chosen for the various parameters (affinity and diffusion coefficient of the buffers, luminal Ca^{2+} concentration) on the kinetic characteristics of these theoretical blips is analyzed.

INTRODUCTION

The Ca^{2+}-dependence of the opening of inositol 1,4,5-trisphosphate ($InsP_3$)-sensitive channels in the endoplasmic reticulum is now believed to play a major role in both elementary and global aspects of Ca^{2+} signalling, in a variety of cell types [4]. The dual effect of Ca^{2+} on channel opening, i.e. fast activation and slower inhibition, has been well characterized in in vitro systems, by $^{45}Ca^{2+}$ flux measurements and electrophysiological measurements of the activity of the $InsP_3$-sensitive Ca^{2+} channels reconstituted in lipid bilayers [2,5]. On the other hand, in vivo observations of the behaviour of these channels suggest that the bell-shaped dependence of their activity on cytosolic Ca^{2+} plays a major role in the regulation of Ca^{2+} in intact cells [4], presumably because the activities of the $InsP_3$-sensitive

Received 7 January 1998
Revised 6 March 1998
Accepted 13 March 1998

Correspondence to: Dr S. Swillens, IRIBHN – ULB, Campus Erasme, route de Lennik 808, B-1070 Brussels, Belgium
Tel: +32 2 555 4160; Fax: +32 2 555 4655. E-mail: swillens@ulb.ac.be

Ca^{2+} channels distributed throughout the cytoplasm may be co-ordinated through Ca^{2+} diffusion. For sufficient stimulatory levels, oscillations and waves can develop [4]. From a theoretical point of view, this feedback effect of Ca^{2+} on the Ca^{2+} releasing activity has been incorporated in many different models, and has accounted for a variety of experimental facts, e.g. oscillations of cytosolic Ca^{2+} and intracellular propagation of Ca^{2+} waves [6–9].

Independently, the potential implications of the fact that the local Ca^{2+} concentration is much higher at the mouth of an open channel than in the bulk cytoplasm gained wide recognition [10–12]. The spatial and dynamic characteristics of these intermediate Ca^{2+} domains were studied for several types of channels [13–21]. Previously, we suggested that these intermediate domains could be responsible for interesting properties of the $InsP_3$-sensitive channel, such as the possibility to generate an incremental detection-like behaviour [22] or long-period Ca^{2+} oscillations [9]. The critical role of endogenous or exogenous Ca^{2+} buffers for such local Ca^{2+} signalling was also recognized [23,24].

Since most models are interested in describing the behaviour of a cell which contains a large population of channels, they are generally based on deterministic kinetic equations. However, it is not clear how the idea of intermediate domains with a high concentration of Ca^{2+} can withstand the explicit consideration of both the stochastic nature of the channel opening and the relatively fast Ca^{2+} diffusion: indeed, it is not unreasonable to anticipate intuitively that such a domain would be washed away by passive diffusion very rapidly after channel closure.

In this work, we have, therefore, attempted to describe in stochastic terms the behaviour of a single $InsP_3$-sensitive channel inserted in a cytosol-like medium with realistic diffusion characteristics. Interestingly, we found that under these conditions, and with minimal hypotheses about the parameters to be used, our simulated channel exhibited bursts of activity, i.e. repetitive openings due to re-activation of the channel by the Ca^{2+} ions flowing through it. The resulting simulated rises in the average Ca^{2+} concentration in a macroscopic volume around the channel were reminiscent of experimentally observed fundamental events in Ca^{2+} release, the so-called 'blips' [1], whose duration had not been understood previously and for which our simulation might thus provide a realistic explanation.

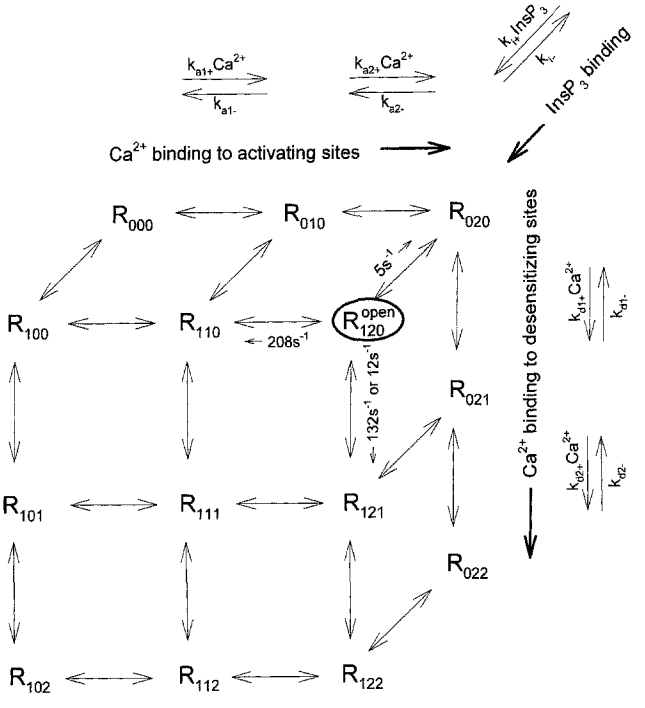

Fig. 1 Model of $InsP_3$-sensitive Ca^{2+} channel. The channel exhibits different states, defined by the absence or the presence of $InsP_3$ and Ca^{2+} in the respective specific binding sites: the symbol R_{ijk} refers to the state of the channel, to which i (0 or 1) $InsP_3$ molecule, j (0, 1 or 2) Ca^{2+} ions (at the activating sites), and k (0, 1 or 2) Ca^{2+} ions (at the desensitizing sites) are bound. The transitions between the different states may be described by a cubic scheme, partially represented in the figure. Ca^{2+} binding to activating and desensitizing sites are shown as horizontal and vertical transitions, respectively. $InsP_3$ binding is represented by transitions between back and front faces of the cube. The life time of the open state (encircled) depends on the kinetics of the three events which, in this scheme, are quantitatively characterized by their first order (for $InsP_3$ dissociation or Ca^{2+} dissociation from the activating site) or pseudo first order (for Ca^{2+} binding to desensitizing sites) rate constants. In the latter case, the value is proportional to the Ca^{2+} concentration at the mouth of the channel: the high and the low values shown correspond to an unitary current of 1.1 pA or 0.1 pA, respectively, under bilayer experimental conditions.

MATERIALS AND METHODS

Operational model for the $InsP_3$-sensitive Ca^{2+} channel

Our aim was to develop an operational model which could account for the following properties of the $InsP_3$-sensitive Ca^{2+} channel: (i) the open probability of the channel exhibits a bell-shaped dependence on cytosolic Ca^{2+} concentration, with a slight positive co-operativity [2]; and (ii) the mean open time of the channel decreases as the Ca^{2+} flux increases [3].

Our basic model is shown in Figure 1. It is based on the existence of a single $InsP_3$ binding site (for simplicity, it is assumed here that $InsP_3$ binding is not co-operative [25]), two activating Ca^{2+} binding sites and two inhibitory or 'desensitizing' Ca^{2+} binding sites. It is assumed that $InsP_3$ binding does not depend on Ca^{2+} binding and that, although Ca^{2+} binding to the activating sites and to the desensitizing sites is co-operative in both cases, there is no allosteric interaction between these different sites. As

shown in Figure 1, R_{ijk} refers to the different states of the channel: i is equal to 1 or 0 depending on whether $InsP_3$ is bound or not to the channel, j represents the number of activating sites occupied by Ca^{2+} (j = 0, 1 or 2), and k represents the number of desensitizing sites occupied by Ca^{2+} (k = 0, 1 or 2). It is assumed that the channel is in the open state only when $InsP_3$ is bound and when Ca^{2+} is present on both activating sites while not present on any of the desensitizing sites, i.e. the open state is R_{120}. The channel is closed in all other situations.

When the channel is open, the Ca^{2+} concentration in the vicinity of the channel is higher than that in the bulk cytosolic phase and, thus, the kinetics of Ca^{2+} association to the desensitizing sites depends on this local concentration at the mouth of the channel (Ca^{2+}_{mouth}). When the channel closes, excess Ca^{2+} disappears by diffusion. In order to simulate Ca^{2+} binding to activatory and desensitizing sites, this local Ca^{2+} concentration at the mouth of the channel must be computed at every instant.

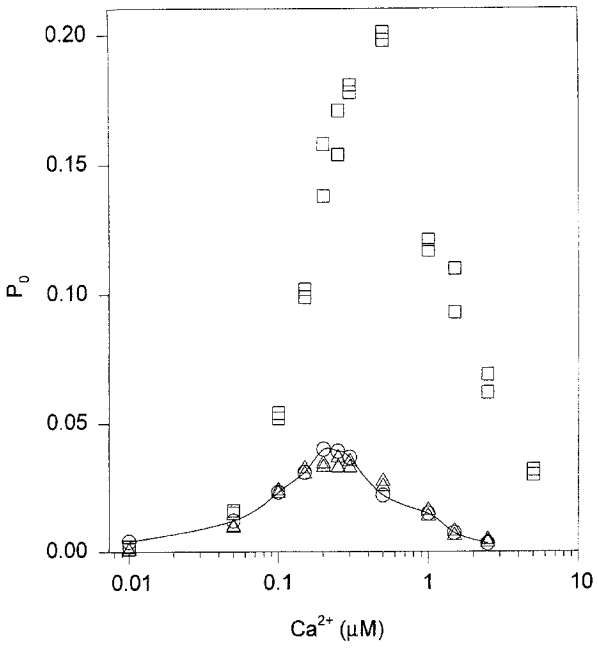

Fig. 2 Stochastic simulation of the model under bilayer conditions: relationship between the channel open probability and the Ca^{2+} concentration in the *cis* chamber. The stochastic simulation of the model proposed in Figure 1 was based on the set of parameters values defined in Table 1, chosen to account for the experimental data illustrated here by circles joined by a solid line [2]. The simulated open probabilities were obtained with an unitary current of either 1.1 pA (triangles) or 0.1 pA (squares).

Stochastic simulation of the channel behaviour

Simulation of the activity of a single channel requires a stochastic approach, which takes random transitions between the different channel states into account. Assuming that the channel is in a certain state at time t, the numerical procedure has to calculate the probability of the different transitions and to determine into which state the channel will transform after a short time interval Δt. This stochastic procedure can be described by using the following example. Let us suppose that all binding sites of the channel are vacant at time t (the channel is in state R_{000}). From this state, the three possible events are: $InsP_3$ binding, Ca^{2+} binding to an activating site, or Ca^{2+} binding to a desensitizing site (the corresponding states into which the channel may transform during a time interval Δt are R_{100}, R_{010} and R_{001}). If interval Δt is sufficiently small to allow at most one transition, the probabilities for the channel to transform into the various possible states within this short time interval are given by:

$$P_{(000\rightarrow100)} \cong k_{i+}[InsP_3].\Delta t \qquad \text{Eq. 1}$$

$$P_{(000\rightarrow010)} \cong k_{a1+}[Ca^{2+}_{mouth}].\Delta t \qquad \text{Eq. 2}$$

$$P_{(000\rightarrow001)} \cong k_{d1+}[Ca^{2+}_{mouth}].\Delta t \qquad \text{Eq. 3}$$

with rate constants defined in Figure 1. Note that the Ca^{2+} concentration referred to in these equations is the local Ca^{2+} at the mouth of the channel (computed as indicated below), not the bulk cytosolic Ca^{2+}. The probability for the channel to remain in its initial state (R_{000}) is equal to:

$$P_{(000\rightarrow000)} \cong 1 - (k_{i+}[InsP_3] + k_{a1+}[Ca^{2+}_{mouth}] + k_{d1+}[Ca^{2+}_{mouth}])\Delta t \qquad \text{Eq. 4}$$

Practically, we chose time intervals Δt short enough to ensure that the probability that the channel remains in the same state after Δt was always higher than 0.95. The interval [0,1] was divided into four sub-intervals, corresponding to the four possible states, interval $[0,P_{(000\rightarrow100)}]$ for R_{100}, interval $[P_{(000\rightarrow100)}, P_{(000\rightarrow100)} + P_{(000\rightarrow010)}]$ for R_{010}, interval $[P_{(000\rightarrow100)} + P_{(000\rightarrow010)}, P_{(000\rightarrow100)} + P_{(000\rightarrow010)} + P_{(000\rightarrow001)}]$ for R_{001}, and interval $[P_{(000\rightarrow100)} + P_{(000\rightarrow010)} + P_{(000\rightarrow001)}, 1]$ for R_{000}. The stochastic procedure randomly generated a number between 0 and 1; the sub-interval which contained this random number then defined the channel state at time t + Δt. The procedure was then reproduced over and over to generate a stochastic succession of channel states.

Three dimensional Ca^{2+} diffusion from a point source

Diffusion in a cytosolic-like medium

Since the present study only considers the activity of a single channel placed in a homogeneous three

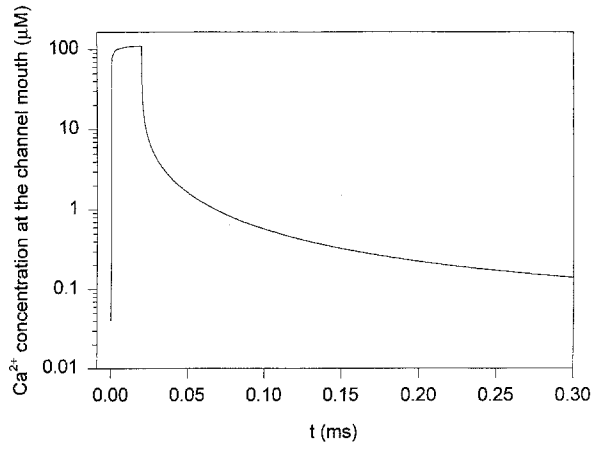

Fig. 3 Ca^{2+} concentration in the vicinity of a Ca^{2+} point source placed in a cytosolic-like medium. The simulation considered a Ca^{2+} point source generating, during 20 μs, a current of 0.1 pA into a cytosolic medium described by a hemispherical space made of 166 shells of 6 nm thickness each. The basal Ca^{2+} concentration was set to 40 nM, and only endogenous buffers were considered, whose characteristics are listed in Table 1. Ca^{2+} diffusion was simulated according to Equation 7. The curve represents the Ca^{2+} concentration in the central hemisphere of 6 nm radius containing the point source. Fitting of the fast component of the decay curve (first 15 μs after source closure) by a two-exponential function gave the following result:

$$Ca^{2+}_{mouth} = 91\ \mu M \exp\left[-\frac{t - t_{closure}}{0.17\ \mu s}\right] + 19\ \mu M \exp\left[-\frac{t - t_{closure}}{5.6\ \mu s}\right] + 0.04\ \mu M$$

dimensional space, Ca^{2+} diffusion was described in spherical co-ordinates: the time-dependent distribution of Ca^{2+} concentration was calculated along the radial direction. For the actual simulation of channel behaviour in a cytosolic environment (Figs 4–7), space discretization was defined as follows: the source was located in a central sphere characterized by a radius Δr; this sphere was surrounded by N successive concentric shells, all with the same thickness equal to Δr. The Ca^{2+} concentration next to the outer shell was kept constant. For simulation of short-range diffusion and evaluation of the local Ca^{2+} concentration at the mouth of the channel (Fig. 3), the space for diffusion consisted of hemispheres only (see Results).

In the absence of buffer, the Ca^{2+} distribution obeys the equation:

$$\frac{\partial C(r,t)}{\partial t} = D_c \nabla^2 C(r,t) + \sigma(r,t) \qquad \text{Eq. 5}$$

where ∇^2 is the Laplacian operator here equal to

$$\frac{2}{r}\frac{\partial}{\partial r} + \frac{\partial^2}{\partial r^2}$$

Table 1 Assumed characteristics for the Ca^{2+} buffers in the cytosol

Buffer	Total concentration (μM)	Ca^{2+} dissociation constant (μM)	Diffusion coefficient ($\mu m^2/s$)
Endogenous			
Stationary	300[a]	10[a]	0
Mobile	50[b]	10[b]	15[c]
Exogenous			
Calcium Green-1	50[a]	0.7[d]	31[e]

[a]Parker et al [27]. [b]Smith et al [20]. [c]Gabso et al [24]

[d]The K_d of Calcium Green-1 is only known under in vitro conditions (about 250 nM [28]). However, 94% of the dye was considered to be bound to cytoplasmic constituents under in vivo conditions, and related dyes under such conditions have a dissociation constant which is several-fold higher than in protein-free solution [29,30]; we thus tentatively estimated that the dissociation constant for Calcium Green-1 to be used was around 700 nM.

[e]We assumed for Calcium Green-1 a diffusion coefficient similar to the one previously measured for the comparable dye Fura–2 [31]; note that the same authors measure a lower diffusion coefficient (15 $\mu m^2/s$) for Indo–1. See also the even lower value (8 $\mu m^2/s$) for Calcium Green-1 itself in muscle fibers [30].

C(r,t) is the Ca^{2+} concentration at time t and at distance r from the center where the source is placed, D_c is the Ca^{2+} diffusion coefficient, and σ(r,t) is the Ca^{2+} influx at the source, i.e. σ(r,t) is different from zero only for r = 0.

For the kind of discretization described above, we approximated the Laplacian operator applied to a function F(r) by operator L, defined as follows:

$$L(F_0) = \frac{1}{\Delta r^2}\left[-2F_0 + 2F_1\right]$$

$$L(F_i) = \frac{1}{\Delta r^2}\left[\left(1 - \frac{1}{i+\frac{1}{2}}\right)F_{i-1} - 2F_i + \left(1 + \frac{1}{i+\frac{1}{2}}\right)F_{i+1}\right] \quad i = 1,2,\ldots N \qquad \text{Eq. 6}$$

where F_i approaches the function F in the i^{th} shell. We checked that these approximations gave results compatible with the analytical solution for a simple system consisting of a constant Ca^{2+} point source placed in an infinite space.

In the presence of Ca^{2+} buffers in the diffusion space, mathematical analysis of Ca^{2+} diffusion is more difficult. Since our study was intended to be semi-quantitative only, we used the rapid buffering approximation proposed by Smith and coworkers [20]. These authors have shown that this approximation is acceptable to mimic physiological buffers, both in the absence and in the presence of moderate concentrations of Ca^{2+} indicator dyes like Calcium Green-1. The procedure calculates Ca^{2+} concentrations at time t + Δt in the central sphere

(C_0) and in the successive shells (C_i, i = 1 to N) as functions of the Ca^{2+} concentrations obtained at time t:

$$C_i(t + \Delta t) = C_i(t) + \Delta t.\beta_i(t)[L(F_i(t)) + \sigma\delta_{i0}] \quad i = 0,1,...N \qquad \text{Eq. 7}$$

with

$$\delta_{00} = 1,\ \delta_{0i} = 0 \text{ for } i > 0 \qquad \text{Eq. 8}$$

$$\beta_i(t) = \left[1 + \frac{K_s B_{s,tot}}{(K_s + C_i(t))^2} + \frac{K_m B_{m,tot}}{(K_m + C_i(t))^2} + \frac{K_e B_{e,tot}}{(K_e + C_i(t))^2}\right]^{-1} \qquad \text{Eq. 9}$$

$$F_i(t) = D_c C_i(t) + D_m \frac{B_{m,tot} C_i(t)}{K_m + C_i(t)} + D_e \frac{B_{e,tot} C_i(t)}{K_e + C_i(t)} \qquad \text{Eq. 10}$$

where indices s and m refer to stationary and mobile endogenous buffers, and index e refers to mobile exogenous buffer; the K_is, $B_{i,tot}$s and D_is are the equilibrium dissociation constants, total buffer concentrations and diffusion coefficients of the mobile buffers, respectively. D_c is the diffusion coefficient of free Ca^{2+} in the cytosol, which was chosen to be equal to 250 $\mu m^2/s$ [26]. Parameters chosen to describe the immobile and mobile endogenous buffers, as well as the mobile exogenous buffer (Ca^{2+} dyes, as mentioned below), are shown in Table 1.

Diffusion in a water-like medium

Under conditions corresponding to an electrophysiological bilayer experiment, where Ca^{2+} diffuses into a Ca^{2+}-buffered *cis* chamber, the stationary Ca^{2+} profile in a hemispherical space can be approached analytically (see [20] for further justifications). At the mouth of the channel, one gets:

$$Ca^{2+}_{mouth} \approx \frac{\sigma}{2\pi D_c r} e^{-\frac{r}{\lambda}} \qquad \text{Eq. 11}$$

where r represents the distance between the Ca^{2+} desensitizing sites and the center of the pore, and λ is a characteristic length which depends on the kinetics of Ca^{2+} binding to the buffer [32]. For instance, taking the experimental conditions from the experiments reported by Bezprozvanny and coworkers [3] into account (i_{Ca}^{2+} = 1.1 pA, 1 mM EGTA), and assuming that D_c = 600 $\mu m^2/s$ characterizes Ca^{2+} diffusion in water [33], we find $\sigma = 5.73 \times 10^{-18}$ mol/s and λ = 632 nm. Since the cytoplasmic part of the $InsP_3$-sensitive Ca^{2+} channel appears to be roughly square-shaped with sides about 12 nm long [34], r should be a few nm, say r = 3 nm. Thus, in such experiments, the computed stationary $[Ca^{2+}_{mouth}]$ turns out to be about 500 μM. A different value can be computed if a different Ca^{2+} current is assumed (see Results).

RESULTS

Stochastic simulation of a single channel under bilayer conditions and determination of parameter values for our model

Our first goal was to define a set of values for the parameters of the model (Fig. 1), allowing to account for the electrophysiological data [2,3] obtained with Ca^{2+} channels incorporated in a planar bilayer. In these experiments, the ionic current flowing through the $InsP_3$-sensitive channel was measured in the presence of a high $InsP_3$ concentration and in the presence of various Ca^{2+} concentrations on the *cis* and *trans* sides of the bilayer: the maximal open probability of a single channel was found to be rather low (around 0.04). With the optimally activating concentration of 200 nM Ca^{2+} in the *cis* chamber, the channel mean open time was found to be either 2.9 or 4.7 ms, depending on whether Ca^{2+} was present (44 mM) or not in the *trans* chamber (Sr^{2+} was added to complement the carrier concentration to 55 mM) [3]. The shorter open time in the presence of luminal Ca^{2+} was interpreted as the consequence of the desensitizing effect of the Ca^{2+} ions flowing through the open channel [3].

According to our model (Fig. 1), the channel closes when any one out of the three following events occurs: (i) dissociation of $InsP_3$; (ii) dissociation of Ca^{2+} from one of the activating sites; or (iii) binding of Ca^{2+} to one of the desensitizing sites. Since the kinetics of these three events are characterized by k_{i-}, k_{a2-} and $k_{d1+}[Ca^{2+}_{mouth}]$, respectively, the two values of the mean open time mentioned above can be used to estimate two of these three kinetic parameters, on the basis of the equation:

$$\text{Mean open time} = \frac{1}{k_{i-} + k_{a2-} + k_{d1+}[Ca^{2+}_{mouth}]} \qquad \text{Eq. 12}$$

where $[Ca^{2+}_{mouth}]$ is the Ca^{2+} concentration in the vicinity of the Ca^{2+} desensitizing site of the open channel. In this equation, the rate of $InsP_3$ dissociation, k_{i-}, can be considered to be 5 s^{-1} as previously measured [35]; in the absence of Ca^{2+} flux in the bilayer experiments, we assume here that $[Ca^{2+}_{mouth}]$ is identical to the bulk Ca^{2+} concentration in the *cis* chamber (200 nM), and in the presence of a 1.1 pA Ca^{2+} flux (once the channel is open), we assume that $[Ca^{2+}_{mouth}]$ is stationary and, because of the size of the channel and the properties of Ca^{2+} diffusion in the *cis* compartment, equal to 500 μM (see Material and methods). From the two corresponding

Table 2 Set of parameter values used to simulate the model defined in Figure 1

	Binding rate constant	Dissociation rate constant
$InsP_3$ site	$k_{i+} = 5 \times 10^6\ M^{-1}s^{-1}$	$k_{i-} = 5\ s^{-1}$
First activating Ca^{2+} site	$k_{a1+} = 8.3 \times 10^7\ M^{-1}s^{-1}$	$k_{a1-} = 250\ s^{-1}$
Second activating Ca^{2+} site	$k_{a2+} = 4.7 \times 10^9\ M^{-1}s^{-1}$	$k_{a2-} = 208\ s^{-1}$
First desensitizing Ca^{2+} site	$k_{d1+} = 2.6 \times 10^5\ M^{-1}s^{-1}$	$k_{d1-} = 57\ s^{-1}$
Second desensitizing Ca^{2+} site	$k_{d2+} = 5.7 \times 10^8\ M^{-1}s^{-1}$	$k_{d2-} = 19\ s^{-1}$

values cited above for the mean open time, we thus conclude that $k_{a2-} = 208\ s^{-1}$ and $k_{d1+}[Ca^{2+}_{mouth}] = 2.6 \times 10^5\ M^{-1}s^{-1}$. Note that since the contributions of the three reactions to closing the channel are in the ratio $k_{i-}/k_{a2-}/k_{d1+}[Ca^{2+}_{mouth}]$, i.e. in the ratio 5/208/132, the rate of Ca^{2+} dissociation from the activating sites appears to play a dominant role, but the contribution of the Ca^{2+} induced desensitizing process is highly significant under these conditions of large luminal Ca^{2+} concentration (44 mM) and, therefore, of large Ca^{2+} flux (1.1 pA) and high Ca^{2+}_{mouth} concentration (500 μM).

The other kinetic parameters describing Ca^{2+} binding cannot be estimated by direct calculation: stochastic simulation of the model is required to define a set of parameter values compatible with the bell-shaped curve describing the channel open probability as a function of the Ca^{2+} concentration in the *cis* chamber [2]. The values presented in Table 2 were found to fit reasonably well the experimental data (compare circles [experimental points] and triangles [simulated points] in Fig. 2; these results were obtained assuming a concentration for $InsP_3$ 10 times higher than the dissociation constant). We repeated twice the numerical simulation in order to show the small variations inherent to stochastic processes. At 200 nM Ca^{2+} in the *cis* chamber, the mean open times corresponding to the simulated experiments were equal to 2.8 and 3.1 ms, respectively, in these duplicate simulations.

It should be kept in mind that the experimental data simulated in Figure 2 were obtained in the presence of 44 mM *trans* (luminal) Ca^{2+}, a concentration which resulted in a large Ca^{2+} flux through the channel. Bezprozvanny and Ehrlich have already pointed out that, under physiological conditions, since the luminal Ca^{2+} concentration was certainly lower, the resulting Ca^{2+} current would be lower; on the basis of an estimated luminal concentration of 2.5 mM, a Ca^{2+} current of about 0.5 pA was predicted [3]. However, several recent studies have shown that in a variety of cell types, the luminal Ca^{2+} concentration is still lower, ranging from 40–700 μM [36–41]. On the basis of an intermediate value of 500 μM, and assuming a linear relationship between the current and the luminal Ca^{2+} concentration in this range of concentrations [3], an even smaller value of 0.1 pA can, therefore, be predicted for the physiological unitary Ca^{2+} current. In this case, the calculation of $[Ca^{2+}_{mouth}]$ (Eq. 11) leads to a value of 46 μM, and stochastic simulation of the model based on this corrected value of luminal Ca^{2+} concentration leads to a second bell-shaped curve for the channel open probability, also shown in Figure 2 (squares). This second curve exhibits a much higher P_o peak value, of about 0.2, and it is slightly shifted to the right compared to the curve obtained with a larger current. This is because Ca^{2+}-induced desensitization is less effective for smaller currents, since the local Ca^{2+} concentration in the vicinity of the open channel is lower: $k_{d1+}Ca^{2+}_{mouth}$ is then only equal to 12 s^{-1}, compared to 132 s^{-1} in the previous case.

Deterministic simulation of Ca^{2+} diffusion in the cytosol

Precise stochastic simulation of the channel behaviour under physiological conditions not only depends on an acceptable choice for the luminal concentration of Ca^{2+} (see squares in Fig. 2), but also depends on the time evolution of the Ca^{2+} concentration at the mouth of the channel. Thus, the actual Ca^{2+} profile in the cytosolic compartment when the channel opens and closes must be computed under physiological conditions. Since the gradient of Ca^{2+} concentration is very steep in the vicinity of the channel mouth, the computation of Ca^{2+} concentration in this region requires a very small spatial grid, in the range of a few nanometers. This high level of discretization increases the computing time enormously. Therefore, the strategy that has been used here was to simulate, once for all under appropriate conditions, the evolution of the Ca^{2+} concentration at the channel mouth, and on the basis of curve fitting, to express this Ca^{2+} concentration as an empirical function of time, for subsequent use in simulations based on a larger spatial grid. Short range diffusion of Ca^{2+} into the cytosol was simulated according to the method of Smith and coworkers [20] (see Methods), using parameters for buffer characterization and composition given in Table 1. We defined the space for Ca^{2+} diffusion close to the channel mouth as an hemisphere made of 166 concentric shells, with a spatial discretization of Δr = 6nm (the choice of an hemispheric geometry is justified by the fact that, for such short-range diffusion, the membrane of the Ca^{2+} reservoir locally creates a quasi-planar barrier to the diffusion of cytosolic molecules).

The basal Ca^{2+} concentration was set equal to 40 nM. Figure 3 shows the kinetics of Ca^{2+} accumulation in the central hemisphere after channel opening (the central hemisphere with its 12 nm diameter was considered to reflect the dimensions of the cytosolic domain of the channel), as well as its decay after channel closure. The Ca^{2+} point source was supposed to contribute a 0.1 pA current (see above). It can be seen that, once the channel opens, the Ca^{2+} concentration very rapidly reaches a rather high value, around 110 μM (characteristic rise time less than 1 μs). It is also apparent that after channel closure, the Ca^{2+} decay curve is multiphasic, with an initial fast decay over the first few microseconds (note the short time scale in Figure 3: Ca^{2+} at the channel mouth drops to submicromolar values within much less than a millisecond). The Ca^{2+} concentration at the channel mouth (in the central sphere of 6 nm radius) is almost indistinguishable from the average Ca^{2+} concentration calculated in a central sphere of 100 nm radius after about 15 μs (not shown). Thus, within this short time period of 15 μs, the Ca^{2+} concentration was fitted to a biexponential function for subsequent stochastic simulations based on a larger spatial grid (the radius of the central sphere will be 100 nm). In those simulations, we will consider that the Ca^{2+} concentration close to the channel mouth (whose estimation is required to compute the probability of Ca^{2+} binding to activating and desensitizing sites) obeys the following rule: once the channel opens, the Ca^{2+} concentration instantaneously reaches its plateau value; when the channel closes, the bi-exponential function (defined in the caption to Fig. 3) describes the fast Ca^{2+} decay. The same simulation was repeated to determine the evolution of Ca^{2+} when 50 μM of an exogenous Ca^{2+}-sensitive dye, Calcium Green-1 (whose assumed properties are also summarized in Table 1) was added to the cytosolic medium, and a new set of parameter values for the bi-exponential function was obtained by curve fitting (result not shown).

Before turning to the actual stochastic simulation of an isolated channel in a cytosolic environment, we also evaluated, with the same deterministic approach as above, whether the channel activity was likely to be detectable under experimental conditions, i.e. when the average Ca^{2+} concentration is measured in a macroscopic volume, of the order of the femtoliter (see below). For this purpose, we evaluated long-range diffusion away from the channel mouth: the space for Ca^{2+} diffusion was now defined as a complete sphere made of 20 concentric shells of 100 nm thickness each (the radius of the largest shell was thus 2 μm; this choice of complete spheres was made because their dimensions now largely exceed the thickness of the tubules of the endoplasmic reticulum). The diffusing space was again supposed to contain an initial basal Ca^{2+} concentration of 40 nM, as well as

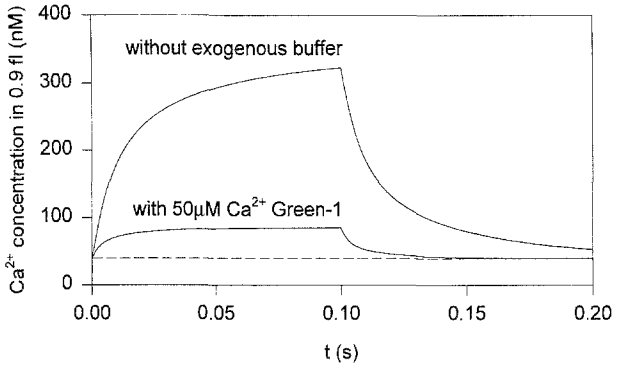

Fig. 4 Ca^{2+} concentration in a macroscopic (0.9 fl) cytosolic volume surrounding a Ca^{2+} point source. The simulation considered a Ca^{2+} point source generating, during 100 ms, a current of 0.1 pA into a cytosolic medium described here by a spherical space made of 20 shells of 100 nm thickness each. The basal Ca^{2+} concentration was set to 40 nM (dashed line). Ca^{2+} diffusion was simulated according to Equation 7. The curves (solid lines) represent the average Ca^{2+} concentration in the six central shells (600 nm total radius), corresponding to a 0.9 fl volume. The curves were obtained assuming an endogenous buffer composition as defined in Table 1, either in the absence or in the presence of 50 μM Calcium Green-1, as indicated.

homogeneously distributed endogenous buffers, defined in Table 1; the same Ca^{2+} source was placed in the center. Since 'elementary' or even 'fundamental' events of $InsP_3$-dependent Ca^{2+} release are nowadays recorded from femtoliter volumes in the presence of Ca^{2+}-sensitive indicator dyes [1], we computed the kinetics of Ca^{2+} accumulation into the 6 central shells after channel opening, as well as its decay after channel closure: these 6 shells with a total radius of 600 nm, correspond to a volume of 0.9 fl. The channel was supposed to provide, during the first 100 ms, a constant Ca^{2+} source (σ) equal to 5.73×10^{-18} mol/s (which corresponds to the 0.1 pA unitary current of the $InsP_3$-sensitive Ca^{2+} channel). Figure 4 shows the results obtained, both in the absence (upper curve) and in the presence (lower curve) of 50 μM Calcium Green-1. In the absence of any exogenous dye, under conditions where the basal Ca^{2+} concentration was 40 nM, the mean Ca^{2+} concentration in the 0.9 fl volume rose to more than 300 nM upon channel opening, and the time required to attain the half maximal amplitude, $t_{1/2}$, was about 11 ms, both in the rising phase, when the current was turned on, and during its decay, current turned off. In the presence of 50 μM Calcium Green-1, which acted as a mobile Ca^{2+} buffer, the amplitude of the Ca^{2+} rise was reduced to about 50 nM above the basal value, and the kinetics of the Ca^{2+} concentration changes were accelerated, as indicated by a $t_{1/2}$ value of about 5 ms. This smaller amplitude of 50 nM is, nevertheless, compatible with the experimentally observed Ca^{2+} signals corresponding to the so-called 'blips' [1,42].

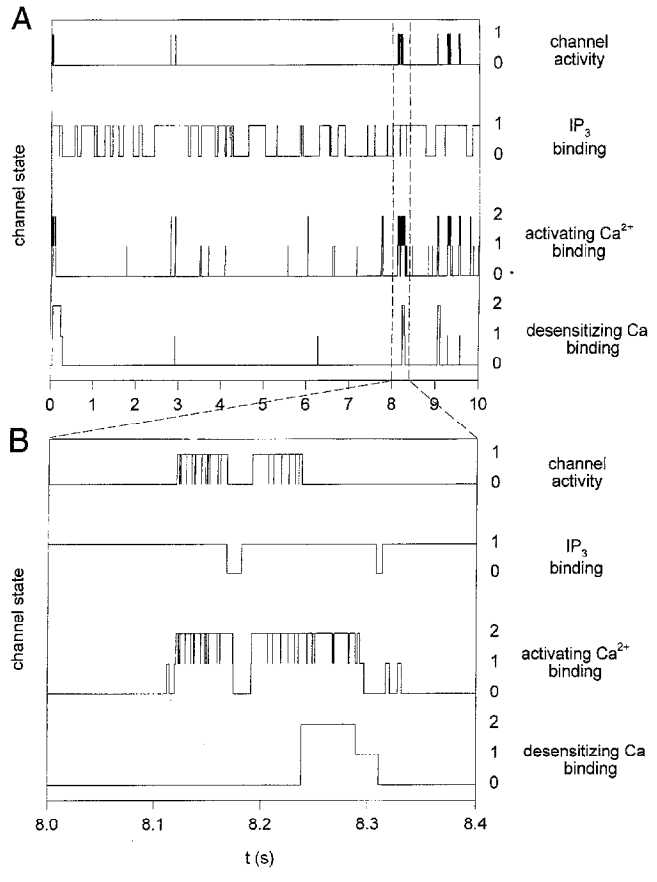

Fig. 5 Stochastic simulation of the model under physiological conditions: evolution of the channel states, with respect to $InsP_3$ and Ca^{2+} binding. The stochastic simulation considered the channel placed in a cytosolic medium described by a spherical space, again made of 20 shells of 100 nm thickness each. The basal Ca^{2+} concentration was set to 40 nM, and only endogenous buffers were considered (with the characteristics indicated in Table 1). The $InsP_3$ concentration was set to its K_d value (1 μM). (**A**) 10 s traces of (i) the activity state (1 and 0 refer to open and closed states, respectively) and of the occupancy of the channel sites by (ii) $InsP_3$, (iii) activating Ca^{2+} ions and (iv) desensitizing Ca^{2+} ions. (**B**) Same traces as in (A), plotted on an expanded time scale.

Stochastic simulation of an isolated channel in the cytosol

The model developed above now allows us to simulate a single channel in a realistic physiological environment. The cytosol was again simulated by considering 20 concentric shells of 100 nm thickness each (the total radius was thus 2 μm), initially containing a basal Ca^{2+} concentration of 40 nM; the diffusing space was supposed to contain physiological concentrations of endogenous buffers, and the Ca^{2+} concentration surrounding the largest shell was maintained at 40 nM. A channel was placed in the center of the sphere, and $InsP_3$ was supposed to be present at a half-saturating concentration. When the channel opened, it contributed a current of 0.1 pA. Figure 5A shows a 10 s run simulating the stochastic transitions between the various states of the channel. As expected from the relatively slow rate of $InsP_3$ dissociation ($k_{i-} = 5\ s^{-1}$), the $InsP_3$ bound state (second line in Fig. 5A) was more stable than the Ca^{2+} bound states (third and fourth lines in Fig. 5A). Ca^{2+} binding to the desensitizing sites (fourth line in Fig. 5A) was a relatively rare event, which generally followed the opening of the channel (first line in Fig. 5A) because of the higher Ca^{2+} concentration at the channel mouth after its opening (in this case, the maximal rate of Ca^{2+} binding to these sites, $k_{d1+}Ca^{2+}_{mouth}$, was 29 s^{-1}).

An attractive finding was that the channel presented bursts of activity, resulting from repetitive openings of the channel (see first line in Fig. 5A, and the same results plotted on an expanded time-scale in Fig. 5B). This phenomenon can be interpreted as the consequence of the high Ca^{2+} concentration at the channel mouth just after channel closure, which makes rebinding of Ca^{2+} at the activating site a likely event. The mean duration of the closed state within one such burst of activity was found to be very short (mean closed time equal to 8 μs).

Stochastic simulation of the time course of Ca^{2+} accumulation in the same spherical volume of 0.9 fl as above was then performed, now letting the channel flicker between its open and closed states. Three distinct traces, simulated in the absence of any indicator dye, are shown in Figure 6A, with a time origin in each case corresponding to the beginning of the activity burst. We previously showed (Fig. 5), that repetitive opening of the Ca^{2+} channel could occur under physiological conditions. It appears in Figure 6A that these repetitive openings lead to transient rises in Ca^{2+} concentration (as measured in our femtoliter spherical volume) which last much longer (up to several tens of milliseconds) than would be expected on the basis of the experimentally found mean open time of the channel (2.9 ms, as measured in bilayer experiments, see above). These long durations in the simulated traces are reminiscent of those in the experimentally observed Ca^{2+} 'blips', corresponding to Ca^{2+} rises in femtoliter volumes of cytosol at low $InsP_3$ concentrations [1] (note that in our simulations of the behaviour of **isolated** channels, the same activity bursts show up both at high and low $InsP_3$ concentrations, but of course with different frequencies). Since an activity burst is produced by channel flickering between the open state R_{120} and the short-lived closed state R_{110}, we defined the burst 'length' as the time interval between the first channel opening and the transition to a state different from R_{120} or R_{110}. This burst length is a random variable which was characterized by the analysis of 300 events. The distributions of the number of channel openings per activity burst and of the burst length are shown in Figure 6B,C, respectively. On average, a burst

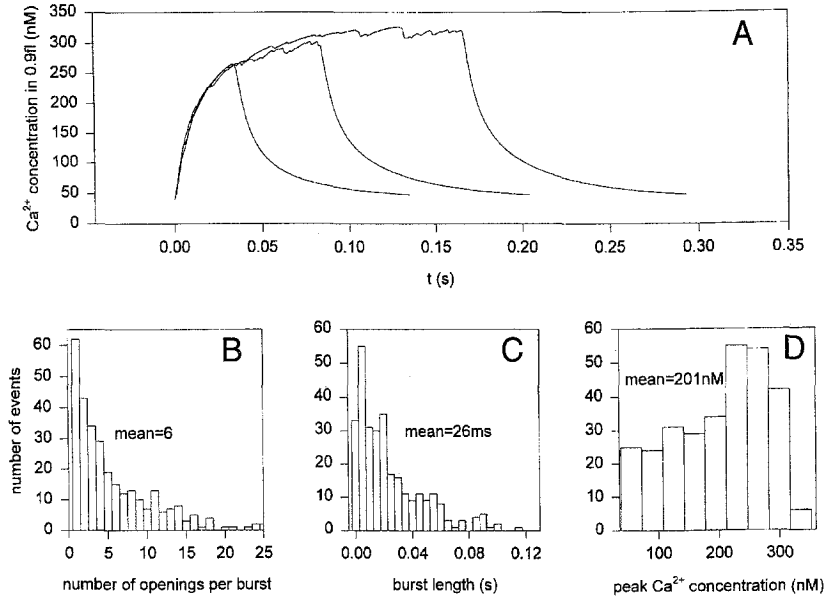

Fig. 6 Stochastic simulation of Ca^{2+} transients in a macroscopic (0.9 fl) cytosolic volume, in the absence of exogenous buffer. The stochastic simulation, performed under the same conditions as in Figure 5, was repeated to generate 300 bursts of channel activity; during each of these bursts, the average Ca^{2+} concentration in a 0.9 fl volume (the 6 central shells) was calculated, and statistical analysis was performed. (**A**) Three activity bursts were selected in order to show the time courses of the corresponding rises in Ca^{2+} concentration, and shown with their time origin aligned. (**B**) Distribution of the number of channel openings during an activity burst. (**C**) Distribution of the burst length. (**D**) Distribution of the maximal or 'peak' Ca^{2+} concentration attained during a burst.

comprised 6 channel openings, and lasted about 26 ms. For the long-lasting bursts, Ca^{2+} concentration attained a plateau value close to 300 nM, which is in agreement with the previous results obtained with the deterministic approach (Fig. 4). Only the shortest bursts of activity were characterized by lower Ca^{2+} amplitudes, because of the time characteristic of Ca^{2+} accumulation. For this reason, the amplitude of the rise in Ca^{2+} concentration during a burst presented a bell-shaped distribution, with a mean value for the peak Ca^{2+} concentration equal to 201 nM (Fig. 6D).

Since Ca^{2+} 'blips' were experimentally observed after including Ca^{2+} fluorescent dyes in the cytosol, we repeated the stochastic simulation of the system under these conditions (Fig. 7). As expected from Figure 4, the inclusion of these additional mobile buffers (50 μM Calcium Green-1) reduced the amplitude of the rise in Ca^{2+} concentration upon channel opening, as well as the average number of channel openings per burst (to about 3) and the length of the burst (to about 14 ms) (compare Fig. 6B,C,D and Fig. 7B,C,D). However, channel repetitive opening was still present, again leading to bursts of activity of much longer duration than expected on the basis of the channel mean open time. Figure 7A demonstrated that the set of parameters used may lead to blips lasting up to several tens of milliseconds and exhibiting an increment in Ca^{2+} concentration of about 40 nM. These simulated results satisfactorily reproduce experimental observations [1]. We thus propose that the blips experimentally observed under physiological conditions in the presence of 50 μM Calcium Green-1 are explained by repetitive opening of a single Ca^{2+} channel.

DISCUSSION

The present simulations were originally performed with the final aim of simulating the mutual influence of channels clustered in what has been called a 'puff' site. This initial aim is still being pursued, but preliminary elaboration of a minimal model for an isolated single channel already led us to an unexpected result, which is the subject of the present report. Under 'realistic' conditions for the buffering capacity of the cytosol, such a simulated isolated channel inside the cytosol was found to display bursts of activity, arising from repetitive openings. In our model, where Ca^{2+} binding to activating sites (or its dissociation) is responsible per se for channel opening (or closing), these repetitive openings are due to the fact that Ca^{2+} ions diffusing away from the channel mouth after its closure in fact diffuse slowly enough to allow rebinding with a significant probability. These simulated results were obtained with a simple molecular model which might not be the exact description of the $InsP_3$-sensitive channel (for instance, $InsP_3$ binding might well be co-operative, and there might be some necessary order in the binding of $InsP_3$ and Ca^{2+} (see [43]).

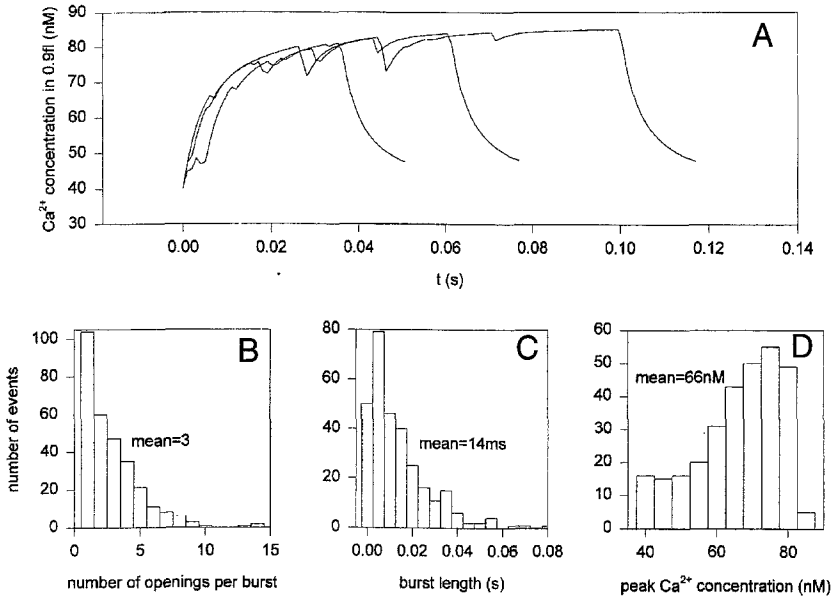

Fig. 7 Stochastic simulation of Ca^{2+} transients in a macroscopic (0.9 fl) cytosolic volume in the presence of 50 μM Calcium Green-1. The stochastic simulation was performed under the same conditions as in Figure 6, except that 50 μM Calcium Green-1 was added to the physiological buffer, with the characteristics shown in Table 1.

Nevertheless, these repetitive openings of the channel are the mere consequence of channel activation by Ca^{2+}, irrespective of the detailed mechanism for this activation. In fact, using a related but different stochastic approach as well as a different model, Stern and coworkers independently arrived at a similar conclusion for the ryanodine-sensitive channel (see Fig. 17 in [44]).

As stated under Results, we suggest that these repetitive openings could explain why previously observed blips, considered to correspond to opening of single channels [1], have an apparent duration much longer than what would be expected on the basis of bilayer characterization of the $InsP_3$-sensitive channel. In fact, from our simulations in Figures 6 and 7, it appears that under in vivo cytosolic-like conditions, i.e. in the absence of exogenous mobile buffers, bursts of channel activity might be even more prominent. These long bursts of activity appear to be simply due to the relatively slow Ca^{2+} diffusion in the cytosol, and do not require for explanation any regulatory difference in the state of the $InsP_3$ receptor under in vitro and in vivo conditions.

As shown in Figure 7D, the distribution of the simulated maximal Ca^{2+} concentrations reached by the blips was bell-shaped. This distribution is reminiscent of the experimental results reported by Parker and coworkers [1]. These authors proposed that the approximately Gaussian shape of the experimental distribution was due either to a roughly constant amount of Ca^{2+} released in each blip, or to the possibility that many undetectable blips had been ignored. In contrast, our simulation shows that such a distribution can be obtained simply as the consequence of the fast rising phase of Ca^{2+} accumulation: thus, although the blip duration and the total amount of Ca^{2+} released during the blip may vary widely, the Ca^{2+} plateau attained by these blip does not change to the same extent.

It must be noted that although all parameter values used here to mimic these blips were deduced from experimental measurements (Table 1), the reasonable agreement observed between simulated behaviour and experimental facts critically depends on these values. In particular, as shown in Figures 6 and 7, the amplitudes and rising times of the simulated blips are highly sensitive to the characteristics assumed for the Ca^{2+} indicator Calcium Green-1. Independently of stochastic simulations, this can also be easily recognized on the basis of simple deterministic simulations (like the one in Fig. 4) of the Ca^{2+} rise resulting from channel opening. Thus, Table 3 explores the effect of making various assumptions for different parameters. Situation (a) corresponds to the hypotheses in Figure 7 (as also used for the lower curve in Fig. 4), in which the simulated blips were obtained assuming that the diffusion coefficient of Calcium Green-1 was equal to the diffusion coefficient experimentally measured for Fura–2 in a cytosolic medium, i.e. 31 $\mu m^2/s$ [31], and that the K_d value for Calcium Green-1 was 2–3 times higher (see e.g. [29,30]) than its value measured in water [28]. Situation (b) corresponds to an assumed K_d value of 270 nM for Calcium Green-1 (as used in [27]), corresponding to the value measured in water without correction for binding

Table 3 Effect of the assumed characteristics of Calcium Green-1 on the kinetics of simulated transient accumulation of Ca^{2+} into a 0.9 fl volume

Situation	Ca^{2+} Green-1 characteristics		Maximal amplitude	$t_{1/2}$
	K_d (nM)	D ($\mu m^2/s$)	nM	ms
a (Fig. 7)	700	31	45	4.5
b	270	31	23	4
c	270	8	81	10
d	270	0	291	34
e (Fig. 6)	no Calcium Green-1		299	11

to cytoplasmic components: in this case, the maximal blip amplitude predicted would drop to only 23 nM above the basal level (situation (b)), and such a low amplitude might be below the detection level. On the other hand, situation (c) corresponds to the situation where, since most of Calcium Green-1 (94% in muscle fibers, according to [30]) appears to be bound to cytoplasmic components and, therefore, does not diffuse in the cytoplasm more rapidly that the components to which it is bound, its apparent diffusion coefficient was assumed to be lower than that in Table 1: for instance, if Calcium Green-1 were to move as slowly as actually measured in muscle fibers, its apparent diffusion coefficient would be reduced down to 8 $\mu m^2/s$ (see Table 3 in [30]), and the maximal Ca^{2+} signal would then increase to 81 nM, while the kinetics of Ca^{2+} accumulation would appear to be slower. Finally, the amplitude of the Ca^{2+} signal would become even higher if the Ca^{2+} indicator were completely immobilized (situation (d)). This would correspond to a mere increase in the concentration of stationary buffers, and, as previously shown [45], such an increase would reduce both the effective current, in terms of free Ca^{2+}, and the effective rate of Ca^{2+} diffusion, with the result that the kinetics of Ca^{2+} accumulation would be slowed down but, the steady state would remain virtually unchanged (compare the characteristics of situation (d) with those obtained in the absence of Ca^{2+} indicator, i.e. situation (e)). Thus, as suggested in previous works [10,20,45], the simulated effect of added Calcium Green-1 under the assumption of Table 1 (situation (a)) appears to be mainly due to its being a mobile buffer: such mobile buffers contribute to faster Ca^{2+} dissipation by diffusion, leading to lower values of Ca^{2+} steady state rises and shorter rise times.

Although the simulated burst lengths shown here are compatible with those of experimental blips, our simulated blips present, in agreement with other theoretical simulations [20,27], Ca^{2+} decay phases much faster than the ones experimentally observed. The characteristic time of a simulated Ca^{2+} decay is about 10 ms (Fig. 7A), whereas experimental decay curves exhibit a characteristic time of about 100 ms [1]. Since the decay rate is only due to diffusion, this discrepancy might point to a misunderstanding of the characteristics of this diffusion. One appealing possibility might be that the cytosolic medium presents physical barriers to macroscopic diffusion. Such a possibility is substantiated by a previous numerical study of the Ca^{2+} dynamics close to the plasma membrane Ca^{2+} channels in smooth muscle cells [17], in which the effect of imposing a barrier to free Ca^{2+} diffusion was investigated. This barrier, possibly corresponding to an intracellular organelle, was defined as a region in which the diffusion coefficient of Ca^{2+} was 10 times lower than in the rest of the cytoplasm, and was supposed to be located about 100 nm away from the plasma membrane. Under such conditions, it was shown that, due to the opening of a single plasma-membrane Ca^{2+} channel, high concentrations of Ca^{2+} developed in the restricted diffusion space between the plasma membrane and the intracellular organelle, and an elevated Ca^{2+} level persisted for 100–200 ms. This interesting possibility has not been included in our model, but would solve the apparent discrepancy mentioned above.

ACKNOWLEDGEMENTS

This study was supported by the Belgian Program on University Poles of Attraction (initiated by the Belgian State, Prime Minister's office, Service for Sciences, Technology and Culture), the Actions de Recherche Concertée Program ARC 94-96 (launched by the Division of Scientific Research, Ministry of Science and Education, French Community of Belgium) and by a CFB-INSERM exchange program. The scientific responsibility is assumed by the authors. GD is Chargé de Recherches at the Belgian FNRS.

REFERENCES

1. Parker I., Yao Y. Ca^{2+} transients associated with openings of inositol trisphosphate-gated channels in *Xenopus* oocytes. *J Physiol Lond* 1996; **491**: 663–668.
2. Bezprozvanny I., Watras J., Ehrlich B.E. Bell-shaped calcium-response curves of Ins(1,4,5)P_3- and calcium- gated channels from endoplasmic reticulum of cerebellum. *Nature* 1991; **351**: 751–754.
3. Bezprozvanny I., Ehrlich B.E. Inositol (1,4,5)-trisphosphate ($InsP_3$)-gated Ca channels from cerebellum: conduction properties for divalent cations and regulation by intraluminal calcium. *J Gen Physiol* 1994; **104**: 821–856.
4. Berridge M.J. Elementary and global aspects of calcium signalling. *J Physiol Lond* 1997; **499**: 290–306.
5. Finch E.A., Turner T.J., Goldin S.M. Calcium as a coagonist of inositol 1,4,5-trisphosphate-induced calcium release. *Science* 1991; **252**: 443–446.
6. Dupont G., Goldbeter A. One-pool model for Ca^{2+} oscillations involving Ca^{2+} and inositol 1,4,5-trisphosphate as co-agonists for Ca^{2+} release. *Cell Calcium* 1993; **14**: 311–322.

7. Sneyd J., Keizer J., Sanderson M.J. Mechanisms of calcium oscillations and waves: a quantitative analysis. *FASEB J* 1995; **9**: 1463–1472.
8. Tang Y., Stephenson J.L., Othmer H.G. Simplification and analysis of models of calcium dynamics based on IP_3-sensitive calcium channel kinetics. *Biophys J* 1996; **70**: 246–263.
9. Dupont G., Swillens S. Quantal release, incremental detection, and long-period Ca^{2+} oscillations in a model based on regulatory Ca^{2+}-binding sites along the permeation pathway. *Biophys J* 1996; **71**: 1714–1722.
10. Stern M.D. Buffering of calcium in the vicinity of a channel pore. *Cell Calcium* 1992; **13**: 183–192.
11. Neher E. The use of fura-2 for estimating Ca buffers and Ca fluxes. *Neuropharmacology* 1995; **34**: 1423–1442.
12. Kasai H., Petersen O.H. Spatial dynamics of second messengers: IP_3 and cAMP as long-range and associative messengers. *Trends Neurosci* 1994; **17**: 95–101.
13. Sherman A., Keizer J., Rinzel J. Domain model for Ca^{2+}-inactivation of Ca^{2+} channels at low channel density. *Biophys J* 1990; **58**: 985–995.
14. Neher E., Augustine G.J. Calcium gradients and buffers in bovine chromaffin cells. *J Physiol Lond* 1992; **450**: 273–301.
15. Imredy J.P., Yue D.T. Submicroscopic Ca^{2+} diffusion mediates inhibitory coupling between individual Ca^{2+} channels. *Neuron* 1992; **9**: 197–207.
16. Rizzuto R., Brini M., Murgia M., Pozzan T. Microdomains with high Ca^{2+} close to IP_3-sensitive channels that are sensed by neighboring mitochondria. *Science* 1993; **262**: 744–747.
17. Kargacin G.J. Calcium signaling in restricted diffusion spaces. *Biophys J* 1994; **67**: 262–272.
18. Monck J.R., Robinson I.M., Escobar A.L., Vergara J.L., Fernandez J.M. Pulsed laser imaging of rapid Ca^{2+} gradients in excitable cells. *Biophys J* 1994; **67**: 505–514.
19. Llinas R., Sugimori M., Silver R.B. The concept of calcium concentration microdomains in synaptic transmission. *Neuropharmacology* 1995; **34**: 1443–1451.
20. Smith G.D., Wagner J., Keizer J. Validity of the rapid buffering approximation near a point source of calcium ions. *Biophys J* 1996; **70**: 2527–2539.
21. Rios E., Stern M.D. Calcium in close quarters: microdomain feedback in excitation-contraction coupling and other cell biological phenomena. *Annu Rev Biophys Biomol Struct* 1997; **26**: 47–82.
22. Swillens S., Combettes L., Champeil P. Transient inositol 1,4,5-trisphosphate-induced Ca^{2+} release: a model based on regulatory Ca^{2+}-binding sites along the permeation pathway. *Proc Natl Acad Sci USA* 1994; **91**: 10074–10078.
23. Zhou Z., Neher E. Mobile and immobile calcium buffers in bovine adrenal chromaffin cells. *J Physiol Lond* 1993; **469**: 245–273.
24. Gabso M., Neher E., Spira M.E. Low mobility of the Ca^{2+} buffers in axons of cultured *Aplysia* neurons. *Neuron* 1997; **18**: 473–481.
25. Watras J., Bezprozvanny I., Ehrlich B.E. Inositol 1,4,5-trisphosphate-gated channels in cerebellum: presence of multiple conductance states. *J Neurosci* 1991; **11**: 3239–3245.
26. Allbritton N.L., Meyer T., Stryer L. Range of messenger action of calcium ion and inositol 1,4,5-trisphosphate. *Science* 1992; **258**: 1812–1815.
27. Parker I., Choi J., Yao Y. Elementary events of $InsP_3$-induced Ca^{2+} liberation in *Xenopus* oocytes: hot spots, puffs and blips. *Cell Calcium* 1996; **20**: 105–121.
28. Eberhard M., Erne P. Calcium binding to fluorescent calcium indicators: calcium green, calcium orange and calcium crimson. *Biochem Biophys Res Commun* 1991; **180**: 209–215.
29. Bassani J.W., Bassani R.A., Bers D.M. Calibration of indo-1 and resting intracellular $[Ca]_i$ in intact rabbit cardiac myocytes. *Biophys J* 1995; **68**: 1453–1460.
30. Zhao M., Hollingworth S., Baylor S.M. Properties of tri- and tetracarboxylate Ca^{2+} indicators in frog skeletal muscle fibers. *Biophys J* 1996; **70**: 896–916.
31. Blatter L.A., Wier W.G. Intracellular diffusion, binding, and compartmentalization of the fluorescent calcium indicators indo-1 and fura-2. *Biophys J* 1990; **58**: 1491–1499.
32. Neher E. Concentration profiles of intracellular calcium in the presence of a diffusible chelator. In: Heinemann U., Klee M., Neher E., Singer W. (eds) *Calcium Electrogenesis and Neuronal Functioning*. Berlin: Springer, 1986; 80–96.
33. Kushmerick M.J., Podolsky R.J. Ionic mobility in muscle cells. *Science* 1969; **166**: 1297–1298.
34. Katayama E., Funahashi H., Michikawa T. et al. Native structure and arrangement of inositol-1,4,5-trisphosphate receptor molecules in bovine cerebellar Purkinje cells as studied by quick-freeze deep-etch electron microscopy. *EMBO J* 1996; **15**: 4844–4851.
35. Hannaert Merah Z., Combettes L., Coquil J.F. et al. Characterization of the co-agonist effects of strontium and calcium on *myo*-inositol trisphosphate-dependent ion fluxes in cerebellar microsomes. *Cell Calcium* 1995; **18**: 390–399.
36. Chatton J.Y., Liu H., Stucki J.W. Simultaneous measurements of Ca^{2+} in the intracellular stores and the cytosol of hepatocytes during hormone-induced Ca^{2+} oscillations. *FEBS Lett* 1995; **368**: 165–168.
37. Combettes L., Cheek T.R., Taylor C.W. Regulation of inositol trisphosphate receptors by luminal Ca^{2+} contributes to quantal Ca^{2+} mobilization. *EMBO J* 1996; **15**: 2086–2093.
38. Hofer A.M., Schulz I. Quantification of intraluminal free [Ca] in the agonist-sensitive internal calcium store using compartmentalized fluorescent indicators: some considerations. *Cell Calcium* 1996; **20**: 235–242.
39. Tanimura A., Turner R.J. Calcium release in HSY cells conforms to a steady-state mechanism involving regulation of the inositol 1,4,5- trisphosphate receptor Ca^{2+} channel by luminal $[Ca^{2+}]$. *J Cell Biol* 1996; **132**: 607–616.
40. Miyawaki A., Llopis J., Heim R. et al. Fluorescent indicators for Ca^{2+} based on green fluorescent proteins and calmodulin. *Nature* 1997; **388**: 882–887.
41. Montero M., Barrero M.J., Alvarez J. $[Ca^{2+}]$ microdomains control agonist-induced Ca^{2+} release in intact HeLa cells. *FASEB J* 1997; **11**: 881–885.
42. Bootman M., Niggli E., Berridge M., Lipp P. Imaging the hierarchical Ca^{2+} signalling system in HeLa cells. *J Physiol Lond* 1997; **499**: 307–314.
43. Dawson A.P. Calcium signalling: how do IP_3 receptors work? *Curr Biol* 1997; **7**: R544–R547.
44. Stern M.D., Pizarro G., Rios E. Local control model of excitation-contraction coupling in skeletal muscle. *J Gen Physiol* 1997; **110**: 415–440.
45. Naraghi M., Neher E. Linearized buffered Ca^{2+} diffusion in microdomains and its implications for calculation of $[Ca^{2+}]$ at the mouth of a calcium channel. *J Neurosci* 1997; **17**: 6961–6973